Macromolecules
ARTICLE

Macromolecules **2009**, *42*, 4539–4546 **4539**
DOI: 10.1021/ma900419q

Novel Surface-Attachable Multifunctional Initiators: Synthesis, Grafting, and Polymerization in Aprotic and Protic Solvents

Miklós Czaun,*[,†,‡,§] László Hevesi,[†] Makoto Takafuji,[‡] and Hirotaka Ihara*[,‡]

[†]*Laboratoire de Chimie des Matériaux Organiques, Facultés Universitaires Notre-Dame de la Paix, 61 Rue de Bruxelles, Namur 5000, Belgium, and* [‡]*Department of Applied Chemistry and Biochemistry, Faculty of Engineering, Kumamoto University, 2-39-1 Kurokami, Kumamoto 860-8555, Japan.* [§] *Present address: Loker Hydrocarbon Research Institute, University of Southern California, Los Angeles, CA 90089-1661.*

Received February 24, 2009; Revised Manuscript Received May 27, 2009

ABSTRACT: Novel surface attachable AIBN type initiators involving mono-/di-/trichlorosilane anchoring groups have been successfully synthesized and grafted onto silica microspheres (average diameter, pore size and surface area are 5 μm, 12 nm, and 300 $m^2\ g^{-1}$ respectively). Graft density of surface-tethered initiators was estimated on the basis of elemental analysis and thermogravimetric measurements giving 0.446, 0.705, and 0.819 group nm^{-2} respectively. Owing to the presence of two anchoring groups newly described initiators can attach to the surface through both ends avoiding the fragment-initiated polymerization in the solution that was considered as a main drawback of asymmetric AIBN-type initiators. Surface-initiated radical polymerization of styrene and *N*-vinyl pyrrolidone has been carried out in toluene and water solutions respectively, giving polymer-silica hybrids. Immobilized polystyrene chains were detached from the surface then the molecular weight and molecular weight distribution was determined by gel permeation chromatography giving 141 200 Da (5.58), 145 700 (5.72) and 149 100 Da (5.94), respectively. The connection between the initiator structure and average molecular weight of degrafted polymers furthermore the effect of possible radical−radical termination reaction on the molecular weight is also discussed.

Introduction

Composite materials consist of inorganic substrates and polymers have attracted much attention due to their numerous practical applications in a variety of fields such as colloid stabilization,[1,2] enzyme immobilization,[3] separation studies[4,5] stimuli responsive materials,[6] etc. Inorganic−polymer hybrids are such materials that involve separate regions dominated by either the inorganic or the polymer component and the resultant hybrid materials display properties that are not linear averages of these regions.[7] Inorganic−polymer composites are widespread not only among artificial materials but vast examples can be found in many living systems as diverse as shells, birds or humans; for example human bones consist of 65−70% of inorganic substances mainly hydroxyapatite and 30−35% of organic materials mostly collagen that is a fibrous protein.[8]

Surface modification of inorganic particles is one of the most effective methods for the fabrication of composite materials. However, inorganic−polymer composites can be classified in many ways (e.g., homogeneity, number of components, the experimental technique of the fabrication, etc.), so we limit our attention to the classifications that distinguish physically adsorbed polymers[9] from the chemically adsorbed ones depending on the kind of interaction between the polymer chains and the surface. Although approaches that do not provide chemical bond between the surface and the polymer matrix, for example *in situ* precipitation of inorganic particles into polymers[10,11] also have great importance, the products obtained in these ways often suffer from severe disadvantages related to thermal or chemical instability that may preclude their practical use in many cases (chromatographic stationary phases or catalyst supports).

Introduction of chemical bonds between the surface and the polymer chains usually improves long-term stability and heat resistance of the composites. Generally, there are two techniques to chemically attach polymers onto inorganic surfaces (1) in "grafting to" method[12] the reactive polymer end groups are chemisorbed to the surface of the inorganic particles and (2) "grafting from" method[13−16] in which polymer chains grow from initiators pregrafted onto the surface. The latter method usually provides higher grafting density because the small monomer molecules have higher mobility while the diffusion of bulky polymers against the concentration barrier established by the already attached polymer chains is hindered.

It must be added here that thin layers deposited by macromolecular plasma chemistry also have a high importance, in particular, those chemically attached to the surface; however, their detailed description is beyond the scope of our article.[17]

Much research has been conducted on the development of new surface-initiated polymerization techniques since Dekking and co-workers had performed the first surface-initiated radical polymerization from clay surfaces.[18,19] These attempts have been fuelled by the high variety of functional groups that may be present in monomers and by the diversity of potential applications of the hybrid materials. Generally, surface-initiated radical polymerization techniques[20] can be divided into two classes: (1) so-called "living" methods such as atom transfer radical polymerization (ATRP),[21] reversible addition−fragmentation chain transfer (RAFT),[22] and nitroxide mediated polymerization (NMP),[23,24] and (2) conventional radical polymerization techniques, where polymerization is initiated by radical initiators having thermally unstable moieties (e.g., azo, peroxo, etc.). The advantage of approaches involved in the first class is the ability to

*Corresponding authors. (M.C.) Fax: +1-213-740-6679. Telephone: +1-213-740-5978. E-mail: czaun@usc.edu. (H.I.) Fax: +81 96 342 3662. Telephone: +81 96 342 3661. E-mail: ihara@kumamoto-u.ac.jp.

Published on Web 06/15/2009

Scheme 1. Comparison between the AIBN-Type Initiators Involving One (a) or Two (b) Anchoring Groups

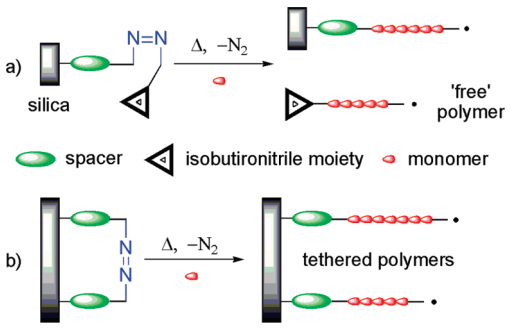

provide polymers (even block copolymers) with low polydispersity while those in the second class are more preferable when control of the molecular weight is not a requirement due to their synthetic ease.

Radical initiators that involve azo linkage as labile group are widely used in solution systems but their application to surface-initiated polymerization has remained a challenging field. A considerable amount of achievements were reported by Nakatsuka[25] and later by Tsubokawa[26] related to the immobilization of 4,4′-azobis(4-cyanopentanoic acid) (ACPA) onto silica that was prefunctionalized with 3-glycidoxypropyltrimethoxysilane and γ-aminopropyltriethoxysilane respectively. Additionally, a comprehensive study has been carried out on the polymerization of vinylic monomers from initiator-functionalized particles that proved the high effectiveness of the surface-attached initiators.

Zhang and co-workers investigated the immobilization of symmetric 4,4′-azobis(4-cyanovaleric acid) derivatives involving two quarternary ammonium groups at both ends into the interlayer spacing of clay layers and the subsequent copolymerization of styrene and MMA.[27] In the same survey, the authors claimed that the amount of polymer brushes on the surface of clay layers could be controlled by the polymerization time.

Particularly noteworthy is the contribution of Prucker and Rühe[14,28] to this field who extensively studied the covalent immobilization of unsymmetrically substituted ACPA onto silica through one chlorosilane anchoring group and their application to surface-initiated polymerization of styrene. Although, high graft densities could be obtained using ACPA-derived initiators that are attached to surface through one "arm", this approach suffers from a significant drawback namely that the liberated molecular fragments obviously cause polymerization in bulk (Scheme 1a). Even though the characterization of "free" polymers isolated from the solution may provide information about the molecular weight of surface attached polymers this phenomenon is encountered as major disadvantage contributing for example to the unnecessary consumption of expensive (and recyclable) monomers or the elevated viscosity of reaction mixtures.

With this problem in mind we have designed and synthesized three, symmetrically substituted ACPA derivatives as novel radical initiators that can be attached to the surface through mono-, di-, or trichlorosilane anchoring groups (Scheme1b). Moreover, the new initiators involve easily hydrolyzable ester functions that allow detaching of polymer chains in order to investigate the molecular weight and molecular weight distribution of the tethered polymers.

Experimental Section

Materials. 4,4′-Azobis(4-cyanovaleric acid) (Aldrich, 75%) was dried under vacuum at room temperature before use. 10-Undecene-1-ol (Aldrich, 98%), dicyclohexylcarbodiimide (Wako, 95%), 4-dimethylaminopyridine (Wako, 99%), and dichloromethane (Nacalai Tesque, 99%) were used as received. Triethylamine (Wako, 99+ %) was distilled from potassium hydroxide. Trichlorosilane (TCI, 97%), dichloromethylsilane (Aldrich, 99%), chlorodimethylsilane (Aldrich, 98%), and platinum(0)-1,3-divinyl-1,1,3,3-tetramethyldisiloxane (Karstedt catalyst) (Aldrich, 0.1 M in xylenes) were used as received. Toluene (Wako, 99%) and diethyl ether (Wako, 99.5%) were distilled from sodium/benzophenone and stored under argon when not in use. Porous silica particles (YMC-GEL) were purchased from YMC Co. Ltd. (Kyoto, Japan) whose average diameter, pore size, and surface area are 5 μm, 12 nm, and 300 $m^2\ g^{-1}$ respectively.

Methods. IR measurements were conducted on a JASCO (Japan) FT/IR-4100 Plus instrument in KBr. For DRIFT measurement accessory DR PRO410-M (JASCO, Japan) was used. Thermogravimetic analyses were performed on a Seiko EXSTAR 6000 TG/DTA 6300 thermobalance in static air from 30 to 800 °C at a heating rate 10 °C min^{-1} using an empty crucible as reference. In order to remove solvent traces each sample was kept under vacuum at 35 °C for 5 h before analysis. Differential scanning calorimetric measurements (DSC) were carried out at a heating rate of 5 °C min^{-1} using a Seiko EXTRA 6000 with a DSC 6200 instrument and an empty pan as reference. A JCM 5700 scanning electron microscope was used for recording SEM images. The accelerating voltage of SEM was 5 kV and the emission current was 12 mA. The GPC chromatographic system consisted of a Jasco PU-2080 Plus HPLC pump with a Rheodine 7725i sample injector having 20 μL loop. A Jasco UV-2075 Plus UV−vis detector was used to determine the relative intensity of elutes. The column temperature was maintained by using Jasco CO-2065 Plus column oven. A personal computer connected to the detector with Chrom Nav 1.8B software was used for system control and data analysis. The separations of samples (10 μL) were performed using HPLC grade chloroform (Wako, 99.7%) as mobile phase at a flow rate 0.5 mL min^{-1}, a TSK Super H−H guard column (4.6×35), TSK-Gel Super HM-M column (6 × 150) and a Jasco DG-2080−53 3-line degasser. For characterization of organic compounds, ^{1}H NMR spectra were recorded on a JEOL JNM-LA400 (Japan) instrument. Chemical shifts (δ) of ^{1}H expressed in parts per million (ppm) relative to the internal standard Me_4Si (δ = 0.00 ppm). Elemental analyses were carried out using a Perkin−Elmer CHNS/O 2400 apparatus.

Syntheses of Undec-2″-enyl-4,4′-azobis-(4-cyanovalerate) (1). First, 1.215 g (7.136 mmol) of 10-undecen-1-ol, 1.620 g (7.850 mmol) of DCC and 0.087 g (0.714 mmol) of DMAP were dissolved in 50 mL of dichloromethane, and then the solution was cooled to 10 °C. Then, 1.25 g (4.460 mmol) of 4,4′-azobis-(4-cyanovaleric acid) was added, and the mixture was stirred in the dark, at room temperature for 24 h. (Note: 4,4′-azobis(4-cyanovaleric acid) was kept under vacuum for 10 h in order to remove the water content. The commercial product contains approximately 20−25% water.) After filtration of the white solid the organic phase was washed with 0.1 M HCl, water and saturated $NaHCO_3$ (three times with each). Organic phase was dried over $MgSO_4$, solvent was evaporated giving a white greasy material (**1**). ^{1}H NMR (400 MHz, $CDCl_3$, δ, ppm): 5.75−5.85 (m, 1H, −CH═), 4.88−5.01 (m, 2H, CH_2═), 4.1 (t, 2H, OCH_2), 2.28−2.55 (m, 6H, CH_2), 2.01−2.07 (q, 4H, $COCH_2CH_2CH_2$), 2.01−2.07 (q, 4H, $COCH_2CH_2$ and CH_2═$CHCH_2$), 1.67−1.74 (s, 3H each, CCH_3), 1.62 (m, 2H, OCH_2CH_2), 1.2−1.4 (b, 12 H, $(CH_2)_6$). FTIR (KBr, ν, cm^{-1}): 3076, 2927, 2855, 2242, 1737, 1640.

General Synthetic Process for 2a−c. First, 0.164 g (0.280 mmol) of undec-2″-enyl-4,4′-azobis-(4-cyanovalerate) (**1**) and 2.0 mL of the corresponding chlorosilane were placed into a round-buttomed flask under inert conditions, and the resulting solution was stirred at room temperature for 5 min. Then 50 μL of Karstedt catalyst was added to the well-stirred solution at 0 °C, and the reaction mixture was allowed to warm up to room temperature. Stirring was continued in the dark, under nitrogen atmosphere for 24 h. Unreacted chlorosilane was evaporated

Scheme 2. Synthesis of Initiators 2a, 2b, and 2c

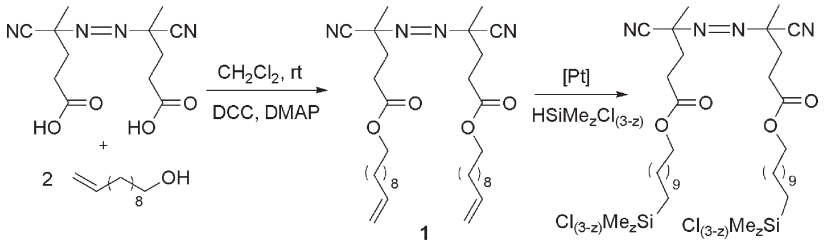

under reduced pressure, leaving a pale yellow viscous liquid that can be used for immobilization without further purification. For characterization, the reaction mixture first was passed through a short layer of silica to remove the catalyst and then chlorosilane was evaporated giving the corresponding silicon coupling agent.

2a. ^{1}H NMR (400 MHz, $CDCl_3$, δ, ppm): 4.1 (t, 2H, OCH_2), 2.35−2.52 (m, 6H, CH_2), 1.68−1.73 (3s, 3H each, CCH_3), 1.2−1.4 (b, 18H, $(CH_2)_9$), 0.81 (t, 2H, $SiCH_2$), 0.4 (s, 6H, $SiCH_3$).

2b. ^{1}H NMR (400 MHz, $CDCl_3$, δ, ppm): 4.1 (t, 2H, OCH_2), 2.35−2.52 (m, 6H, CH_2), 1.68−1.73 (3s, 3H each, CCH_3), 1.49 (m, 2H, $Si-CH_2-CH_2$), 1.2−1.4 (b, 16H, $(CH_2)_8$), 1.13 (t, 2H, $SiCH_2$), 0.77 (s, 3H, $SiCH_3$).

2c. ^{1}H NMR (400 MHz, $CDCl_3$, δ, ppm): 4.1 (t, 2H, OCH_2), 2.35−2.52 (m, 6H, CH_2), 1.68−1.73 (3s, 3H each, CCH_3), 1.4 (m, 2H, $SiCH_2$), 1.2−1.4 (b, 18H, $(CH_2)_9$).

Immobilization of Initiators 2a−c onto Silica. First, 0.6 g of silica was suspended in 6 mL of toluene and sonicated for 15 min. Then 0.28 mmol of initiator in 5 mL of toluene was added under nitrogen atmosphere and the suspension was stirred for 5 min. Then triethylamine was added, and the stirring was continued for 24 h. Silica particles were filtered and washed with toluene, methanol, water and methanol (each 3 ×) and kept under vacuum prior to characterization. Note: the weight of triethylamine (m_{TEA}) was calculated as follows: $m_{TEA} = 1.1 \times n \times N \times 101.19$, where n is the amount of initiator (mol) and N is the number of chlorine atoms per molecule (e.g., $N = 6$ for **2c**).

Sil-**2a**: DRIFT (KBr, ν, cm^{-1}): 2993, 2928, 2856, 1738. Anal. Found: C, 8.84; N, 0.87.

Sil-**2b**: DRIFT (KBr, ν, cm^{-1}): 2992, 2962, 2927, 2858, 1738. Anal. Found: C, 12.47; N, 1.47.

Sil-**2c**: DRIFT (KBr, ν, cm^{-1}): 2989, 2969, 2929, 2857, 1738. Anal. Found: C, 13.41; N, 1.86.

Surface-Initiated Polymerization of Vinylic Monomers from Sil-2a−c. First, 0.1 g of initiator-grafted silica was dispersed and sonicated in a mixture of 2 mL of solvent (toluene or water) and 2 mL of monomer (styrene or *N*-vinyl 2-pyrrolidone). The suspension was deoxygenated by three freeze−pump−thaw cycles and then was immersed in an oil bath preheated to 80 °C. After 24 h reaction time the suspension was filtered and particles were repeatedly washed with toluene and chloroform (for St) alternatively with water and methanol (for NVP).

General Procedure for Degrafting of PSt from PSt-Grafted Silica Particles. First, 0.4 g of PSt-grafted silica was suspended in 25 mL of toluene and 0.020 g (0.105 mmol) *p*-toluenesulfonic acid in 3 mL of methanol was added and the suspension was refluxed for 24 h. The reaction mixture was allowed to cool to room temperature, and 10 mL of toluene was added. After filtration, the filtrate was concentrated under vacuum and precipitated into methanol giving 25−30 mg of white powder. ^{1}H NMR (400 MHz, $CDCl_3$, δ, ppm): 1.2−1.9 (m, CH_2 and CH), 6.3−7.2 (m, Ph). FTIR (KBr, ν, cm^{-1}): 3082, 3060, 3026, 2923, 2851, 1740 (ester C=O), 1602, 1493, 1451, 756, 698.

Results and Discussion

Synthesis of Silane Coupling Agents. The novel AIBN-type initiators were synthesized in two steps: (1) the indirect esterification of azobis(4-cyanovaleric acid) with 10-undecen-1-ol in the presence of dicyclohexylcarbodiimide (DCC) and 4-dimethylaminopyridine (DMAP) followed by (2) addition of mono/di/trichlorosilanes to the terminal carbon−carbon double bonds (Scheme 2). The hydrosilylation reaction of azobis(10-undecenyl-4-cyanovalerate) (**1**) with the corresponding chlorosilanes in the presence of Karstedt catalyst solution provided exclusively the anti-Markovnikov addition products: azobis[11′′-(chlorodimethylsilyl)-undecyl-4-cyanovalerate] (**2a**), azobis[11′′-(dichloromethylsilyl)-undecyl-4-cyanovalerate] (**2b**) and azobis[11′′-(trichlorosilyl)-undecyl-4-cyanovalerate] (**2c**).[15] Conversion of unsaturated esters to the corresponding chlorosilanes was monitored by the disappearance of the multiplet around 5.8 ppm attributed to methyne protons. Alternatively, in the cases of **2a** and **2b**, the hydrosilylation reactions were followed by the appearance of methyl signals at 0.40 and 0.77 ppm assigned to $SiCH_3$ and $Si(CH_3)_2$ moieties respectively. The obtained silane coupling agents and the unsaturated ester were characterized by ^{1}H NMR and FTIR spectroscopy. ^{1}H NMR spectra are shown in the Supporting Information (Figures S1−S4).

Grafting of Initiators 2a−c onto Silica Particles. Initiators **2a−c** were immobilized onto mesoporous silica particles (Scheme 3) in a mixture of dry toluene and triethylamine giving initiator-grafted silica particles Sil-**2a**, Sil-**2b**, and Sil-**2c**, respectively. It is well-known that di- and trichlorosilanes can be attached through two or three siloxane bonds to the substrate but also may react with each other prior to the immobilization *viz*. silica surface and solvents always contain some moisture. Hydrolysis and subsequent condensation of silane coupling agents may lead to the formation of cross-linked silane multilayers where not all initiator molecules are directly connected to the surface but a part of them are attached via other immobilized initiators. Considering the above discussion, detailed structural characterization of the initiator thin layer must be carried out, as is presented in the next section.

Characterization of Initiator-Grafted Silica Particles. Elemental analysis (C, H, N), thermogravimetric analysis (TGA), diffuse reflectance infrared Fourier transform spectroscopy (DRIFT), differential scanning calorimetry (DSC), and scanning electron microscopy (SEM) was used to characterize initiator- and polymer-grafted silica particles.

The graft densities (δ) of silane coupling agents (**2a−c**) on silica particles were determined according to eq 1 from the carbon content of the hybrid giving the values of 221, 351, and 407 μmol g^{-1} respectively. In eq 1, C% is the carbon content of the immobilized initiator on the basis of elemental analysis, C_{in}% and MW are the calculated carbon content and the molecular weight of the corresponding initiator without Si and Cl atoms. Using eq 2 graft densities of **2a - c** were translated to area densities as 0.446, 0.705, and 0.819 group nm^{-2} in the same order. (S is the surface area of silica

Scheme 3. Immobilization of Initiator 2a, Surface-Initiated Polymerization of Vinylic Monomers from Sil-2a and Degrafting of Tethered Polymers

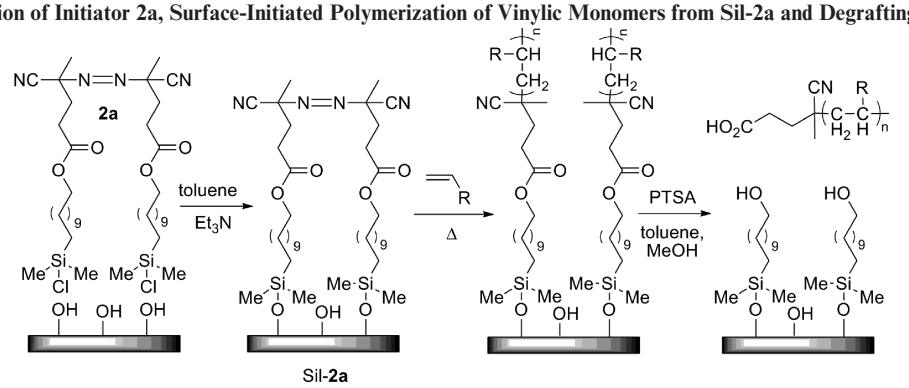

particles; in present case $S = 300\ m^2\ g^{-1}$.

$$\boldsymbol{\delta} = 10^6 \frac{\frac{C\%}{C_{in}\%}}{MW} \times \frac{1}{1 - \frac{C\%}{C_{in}\%}}\ (\mu mol\ g^{-1}) \quad (1)$$

$$\Gamma = \boldsymbol{\delta} \times S\ (\mu mol\ m^{-2}) \quad (2)$$

These area densities are approximately half of those were previously reported by Rühe[14] for asymmetric mono-, di-, and trichlorosilyl azo initiators immobilized onto silica particles (1.11, 1.44, and 1.61 group nm^{-2}) that were attached to the surface through one anchoring group instead of two anchoring groups. This particular difference in area densities is most likely results from the fact that initiators **2a**−**c** are approximately twice as bulky as the unsymmetric ones. Consequently, they occupy a nearly twice larger area on the surface. Obviously, after the cleavage of all azo groups in the initiator molecules the grafting densities can be considered practically the same as reported for unsymmetrical initiators.[14] Considering this evidence, it can be concluded that the surface coverage of Sil-**2a**−**c** reached the maximal value allowed by the bulk of initiators **2a**−**c**. The amount of immobilized initiator or polymeric material in inorganic−organic composites can be easily monitored by thermogravimetric analysis. However, if one intends to translate the differences in weight retentions into graft density one should interpret the TGA curves carefully. Figure 1 displays the TGA curves of bare silica (a) and Sil-**2a**−**c** (b−d). Bare silica particles were found to have 7% weight loss in the temperature range from 30 to 800 °C due to the loss of physically adsorbed water and partly due to the chemical dehydroxylation occurring at higher temperatures.[29] TGA curve of Sil-**2a** (b) and Sil-**2b** (c) plateaued at 130 °C showing weight loss of 1.9 and 2.3% respectively due to the thermal decomposition of azo groups and partly due to evaporation of the adsorbed water while Sil-**2c** lost 3.1% its original weight up to the same temperature. However, we cannot stress enough that it is rather difficult to extract the possible contribution of the surface adsorbed water to the weight loss from the decomposition of azo moieties. Considering the above discussion it is likely that the subtraction of the weight retention of initiator-grafted silica at 800 °C from the weight retention of bare silica leads to false (obviously lower) graft densities because the surface modification altered the hydrophilicity of silica and different amount of water may be adsorbed on it. Even considering the plateaus (130 °C) in the TGA curves of Sil-**2a**−**c** as references still lead to false values since this calculation still does not take into account the weight loss in course of the degradation of the azo moieties. Indeed, the comparison between graft

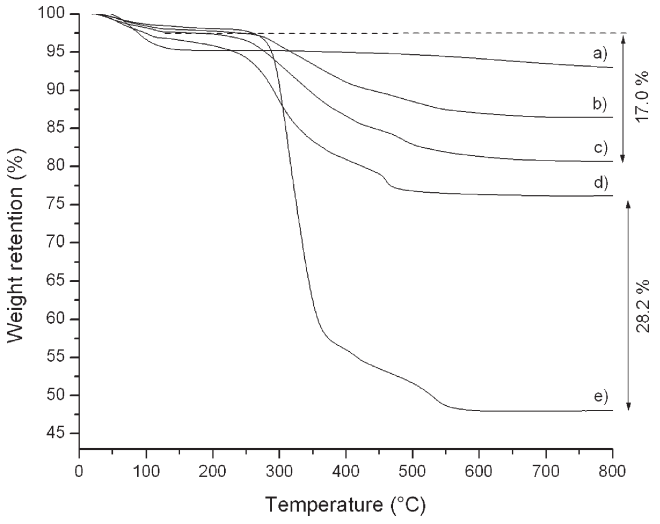

Figure 1. TGA curves of (a) bare silica, (b) Sil-**2a**, (c) Sil-**2b**, (d) Sil-**2c**, and (e) Sil-PS_{2c}.

densities based on TGA and elemental analysis showed significant deviations. In order to clarify this apparent discrepancy we invented a formula (eq 3) for the calculation of graft densities on the basis of TGA measurements in that volatile content of initiator-grafted particles is corrected by the nitrogen content (N_{azo} %) attributed to azo group. $N_{azo}\% = 28/MW$, WR_1 and WR_2 are the weight retentions at 800 and 130 °C, respectively, where plateaus were observed. Not surprisingly, the outcome of calculations using eq 3 gave graft (215, 356, and 486 $\mu mol\ g^{-1}$) and area densities (0.434, 0.717, and 0.867 group nm^{-2}) very similar to those based on elemental analysis (Table 1).

$$\boldsymbol{\delta} = \frac{(WR_1 - WR_2) \times (1 - N_{azo}\%)}{MW} \times \frac{1}{WR_2}\ (\mu mol\ g^{-1}) \quad (3)$$

Differential scanning calorimetric (DSC) investigation of initiator-grafted silica particles was carried out to gain insight into the thermal behavior of the immobilized azo initiator. Thermal decomposition of initiator **2c** was monitored in the temperature range from −15 to +160 °C at a heating rate of 5 °C min^{-1} (Figure 2). While in the first heating process the intensive peak at 114 °C due to the degradation of azo bond is apparent, in the second cycle the lack of this peak clearly indicates that the cleavage of azo moiety is complete. In order to demonstrate the thermal instability of the immobilized initiators in a practical point of view 0.1 g Sil-**2c** was suspended in toluene and stirred at 90 °C under N_2 atmosphere for 12 h.

Table 1. Graft and Area Densities of Initiator 2a−c on Silica Calculated from Elemental Analysis and TGA Compared with Similar Examples in the Literature

	graft and area densities					
	2a		**2b**		**2c**	
method	(μmol g^{-1})	(group nm^{-2})	(μmol g^{-1})	(group nm^{-2})	(μmol g^{-1})	(group nm^{-2})
CHN[a]	221	0.446	351	0.705	407	0.819
CHN[b]	**442**	**0.891**	**702**	**1.409**	**814**	**1.638**
TGA[c]	215	0.434	356	0.717	486	0.867
DSC[d–f]	**525**[d]	**1.108**[d]	**680**[e]	**1.439**[e]	**760**[f]	**1.608**[f]

[a] Calculated by using eq 1 and 2. [b] Graft- and area densities calculated from CHN were multiplied by two (μmol of anchoring group per g or number of anchoring groups per nm^2). [c] Calculated by using eq 3. Note: These values were reported as graft and area densities for asymmetric ACPA derivatives. [d] Monochloro ACPA derivatives. [e] Dichloro ACPA derivatives. [f] Trichloro ACPA derivatives.[14]

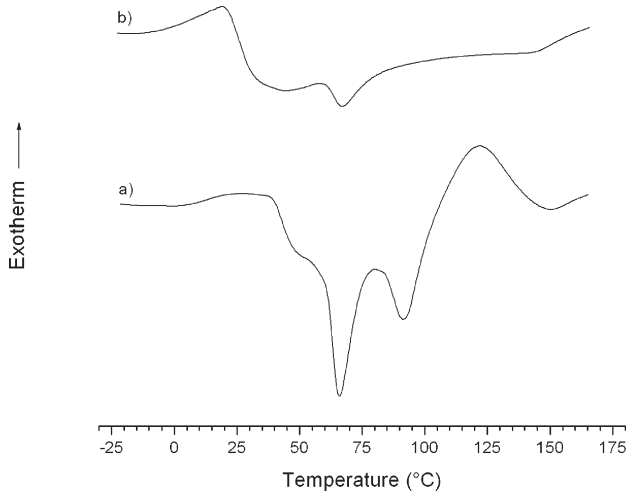

Figure 2. DSC traces of Sil-**2c**: (a) first and (b) second heating process.

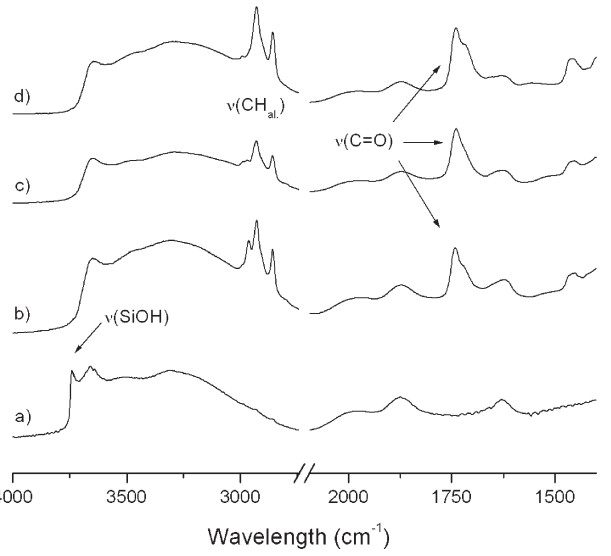

Figure 3. DRIFT spectra of (a) bare silica, (b) Sil-**2a**, (c) Sil-**2b**, and (d) Sil-**2c**.

The TGA curves (Figure S5) show that the thermally treated Sil-**2c** contains 2.7% less volatile material due to the liberation of nitrogen gas from azo moieties. Similarly, while elemental analysis of Sil-**2c** showed 1.86% nitrogen content only 0.77% nitrogen could be measured after the decomposition of an azo group. Surprisingly, the polymerization of St using the thermally treated Sil-**2c** resulted in a few percentage attached polymer. At first sight it seems unusual that radical polymerization takes place from deactivated initiator-grafted silica, however several examples of similar phenomenon can be found in the literature. As it was reported by Meier et al. that the decomposition and subsequent disproportionation of tethered AIBN-type initiators leads to the formation of unsaturated products that then may act as comonomers in the thermally induced polymerization of styrene.[30]

Diffuse reflectance infrared Fourier transform (DRIFT) spectroscopic analysis provides evidence concerning the structure of the molecules immobilized on the surface of inorganic materials. Figure 3 displays the DRIFT spectra of bare silica (a) and initiator-grafted silica particles (b-d). Successful grafting of the silane coupling agents **2a−c** is indicated by the antisymmetric and symmetric streching vibrations of CH_2 groups (2928 and 2856 cm^{-1}) and by the intensive peak at 1737 cm^{-1} due to the stretching vibration of carbonyl groups. Disappearance of the characteristic signal of the surface OH groups[31] at 3739 cm^{-1} further confirmed the grafting of radical initiators.

Surface-Initiated Polymerization from Initiator-Grafted Silica Particles. After appropriate purification as detailed in the Experimental Section the initiator-immobilized silica particles Sil-**2a−c** were used as macroinitiators for surface-initiated radical polymerization of vinyl monomers such as the water insoluble styrene (St) and the water-soluble *N*-vinyl 2-pyrrolidone (NVP) (Scheme 2) under experimental conditions indicated in Table 2. First Sil-**2a−c** were suspended in a mixture of St and toluene (1:1) and then the reaction mixture was degassed by three freeze−pump−thaw cycles. The polymerization reactions were conducted at 80 °C under N_2 atmosphere for 24 h. The resultant silica particles were filtered, repeatedly washed with warm toluene and chloroform and dried under vacuum giving PS-grafted silica particles. For convenience, the hybrid materials derived from polymerization of styrene using Sil-**2a−c** are abbreviated as Sil-PS$_{\mathbf{2a}}$, Sil-PSt$_{\mathbf{2b}}$, and Sil-PSt$_{\mathbf{2c}}$, respectively. In order to isolate the "free" polymers formed in solution the first filtrate was combined with those received during the washing process. The solution was concentrated under vacuum and precipitated into methanol. Finally, the obtained white solids were dissolved in chloroform and reprecipitated into methanol.

Table 2. Weight Percentage of Tethered Polymers on Silica Particles

	weight percentage of tethered polymers (%)[a]		
monomer/solvent	**2a**	**2b**	**2c**
styrene/toluene[b,c]	29.5	31.7	28.2
NVP/water[b,d]	15.0	17.4	21.6

[a] Based on TGA. [b] Monomer:solvent = 1:1, particle loading = 0.1 g/4 mL, 80 °C, N_2. [c] [St] = 4.35 M. [d] [NVP] = 4.68 M.

TGA measurements were carried out to estimate the amount of the tethered polymers on the surface of silica particles (Figure 1, curve e). Comparison between the weight

retentions of Sil-PSt_{2a}, Sil-PSt_{2b}, and Sil-PSt_{2c} and the corresponding initiator-grafted particles revealed that the silica−polymer hybrids contained 29.5, 31.7, and 28.2% PSt respectively (Table 2) indicating that relatively high amounts of polymeric materials could be attached to silica particles using Sil-**2a**−**c** as macroinitiators.

When NVP was polymerized, Sil-**2a**−**c** were suspended in the mixture of the monomer and water (1:1); otherwise, the reaction conditions were the same as described for the polymerization of St. After filtration, the particles were purified by washing with water and methanol and then dried under vacuum prior to characterization. The polymerization of NVP resulted in surface-attached PNVP in yields varying from 15.0% to 21.6% as presented in Table 2. The highest yield of surface-attached PNVP (26.7%) was obtained in an exceptional case when no solvent was used, the initiator-grafted particles (Sil-**2c**) were suspended in pure NVP. It should be noted here that SEM investigation of these Sil-PNVP particles revealed the presence of insoluble, most likely cross-linked domains precluding the separation of the hybrid particles from each other and the formation of a fine suspension (Figure S6). Most probably, the relatively high grafting density of **2c**, the lack of solvent and the noncontrolled feature of the polymerization resulted in high concentration of propagating radicals that might undergo radical termination reactions giving nonsoluble cross-linked network.[32]

Further characterization of polymer-grafted particles was performed using infrared spectroscopy (Figure 4). The DRIFT spectrum of Sil-$PNVP_{2c}$ (d) is the superposition of the spectra of the three components: silica gel (a), initiator-grafted silica (b), and PNVP (c). Two broad peaks could be observed at 2922 and 1675 cm^{-1} attributed to CH vibration and carbonyl stretching vibration of the pyrrolidone moiety, respectively. As a clear evidence of the immobilization of PSt onto silica particles two groups of intense signals due to the aromatic CH stretching (3082−3001 cm^{-1}) and the skeletal vibrations of the benzene ring (1601, 1493, and 1452 cm^{-1}) could be detected. Additionally, a bending vibration at 699 cm^{-1} and three signals with low intensity at 1945, 1872, and 1805 cm^{-1} assigned to overtone vibrations of one substituted benzene ring could also be observed.

In order to gain insight into the molecular weight and molecular weight distribution of polymers prepared on the surface, the immobilized PSt was degrafted from Sil-PS_{2a}, Sil-PS_{2b} and Sil-PS_{2c} by transesterification (Scheme 3) similarly to a previously reported procedure.[14] Polymer grafted silica samples were refluxed in the mixture of toluene and methanol (25:3) in the presence of *p*-toluenesulfonic acid (PTSA) for 24 h (see the Experimental Section). The isolated white powders were investigated by FTIR, ^1H NMR spectroscopy and gel permeation chromatography (GPC). Only one representative example of the ^1H NMR and FTIR spectra is shown since all the degrafted PSt samples were found to be identical. Figure 5 depicts the FTIR spectra of degrafted PSt (a), "free" PSt (b) isolated from the filtrate of polymerization reaction and an authentic sample of PSt (c). In the comparison of spectra a−c let us conclude that spectra a and b are identical with that obtained for authentic PSt except a slightly more intensive absorption band in spectrum a at 1740 cm^{-1} partly due to carbonyl stretching vibration of methyl-(4-cyano-pentanoate) moiety. It is well-known that PSt has a weak absorption band at 1745 cm^{-1} attributed to an overtone vibration as it can be seen in spectra b and c. Nevertheless, it is conspicuous that in spectrum a the intensity of the peak at 1740 cm^{-1} is higher because this peak can be assigned to the overlap of overtone and carbonyl vibration. Additionally, the ^1H NMR spectrum of the detached polymer is also identical to that of authentic PSt as it is shown in Figure S7.

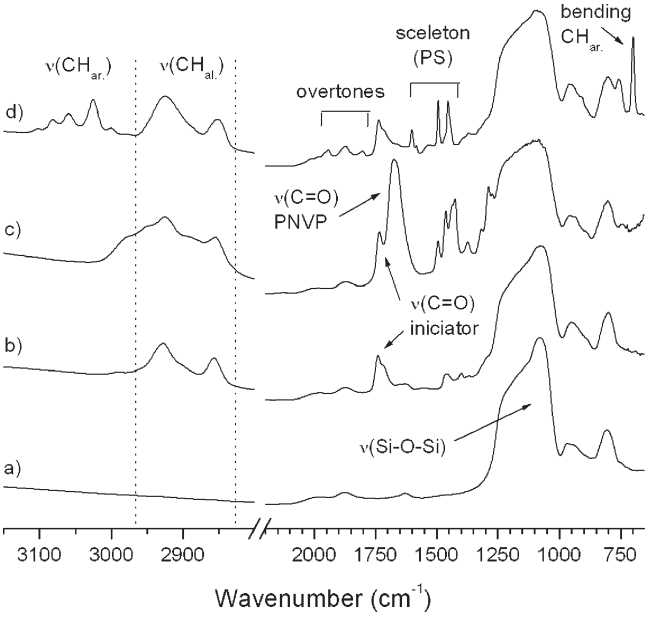

Figure 4. DRIFT spectra of (a) bare silica, (b) Sil-**2c**, (c) Sil-$PNVP_{2c}$, and (d) Sil-PSt_{2c}.

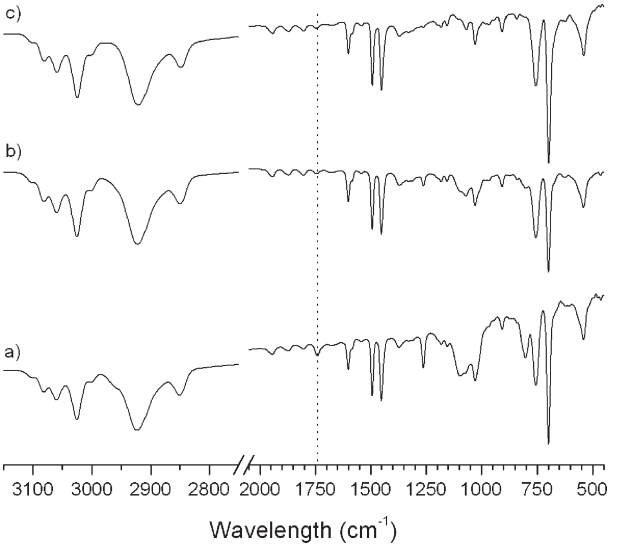

Figure 5. FTIR spectra of (a) degrafted PSt, (b) "free" PSt, and (c) an authentic sample of PSt.

Table 3. M_w and PDI of Degrafted PSt and Area Densities of Polymer-Grafted Silica Particles

polymer-grafted silica	M_w (Da)	PDI	area density (group nm^{-2})
Sil-PSt_{2a}	141 200	5.58	0.0088
Sil-PSt_{2b}	145 700	5.72	0.0089
Sil-PSt_{2c}	149 100	5.94	0.0091

GPC measurement of the polymer detached from Sil-PS_{2a}, Sil-PS_{2b}, and Sil-PS_{2c} resulted in the weight average molecular weight (M_w) and polydispersity (PDI) of 141 200 Da (5.58), 145 700 Da (5.72), and 149 100 Da (5.94) respectively (Table 3). Notably, the M_w values are consistent with that reported by Prucker and Rühe using non symmetric ACPA derivative as initiator (≈10^5 Da). The relatively low

Scheme 4. Termination Reactions in Surface-Initiated Radical Polymerization

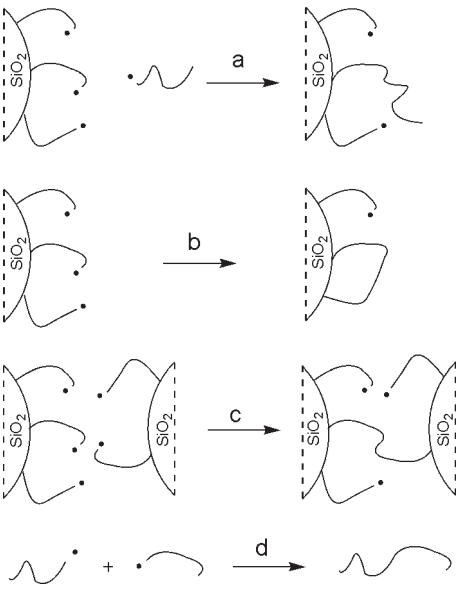

area densities of polymer-grafted silica particles (0.0088−0.0091 group nm^{-2}) calculated from the corresponding polymer content and M_w values indicate that only 10% of the grafted initiators successfully started a polymerization reaction. The low radical efficiency can be explained as a consequence of the favored radical recombination since the noncontrolled cleavage of azo bonds may cause high radical concentration and elevated viscosity close to the surface.

It is particularly noteworthy that the M_w and PDI of PSt isolated directly from the reaction mixture after polymerization was also determined by GPC (115 600 Da and 8.23), giving lower values than the molecular weight of degrafted PSt. Usually, the differences between the molecular weight of surface polymers and bulk polymers are more significant due to the termination reactions between surface attached propagating radicals and "free" propagating chains in solution. One can easily imagine that the termination depicted in Scheme 4a increases the molecular weight of surface-attached polymers while it does not have any influence on those propagating in the solution.[28,33] This type of radical−radical termination often results in larger differences between the molecular weights of "free" and tethered polymers when non symmetric azo type initiators are used especially if the substrate has high surface area. In the present case, although the surface area of silica substrate is relatively high (300 $m^2\ g^{-1}$) the concentration of radical species in solution that formed in the course of homolytic cleavage of the azo bond is very low (theoretically zero) because **2c** is immobilized through two anchoring groups. It is obvious from the above discussion that the termination reactions between tethered propagating radicals cannot be neglected under special conditions (e.g., high particle loading and high graft density of the initiator or solvent free polymerization) as it was confirmed by the formation of insoluble domains of PNVP on the silica surface.

Conclusions

We presented herein the synthesis of a novel family of surface attachable radical initiators derived from 4,4′-azobis(4-cyanopentanoic acid) (ACPA). The synthetic process consists of the esterification of ACPA with 10-undecen-1-ol followed by hydrosilylation of the carbon−carbon double bonds. The new initiators have been immobilized onto silica particles and applied as initiators for the surface-initiated polymerization of both water-soluble and water insoluble vinylic monomers such as *N*-vinyl pyrrolidone and styrene. In summary, our data demonstrated the following:

(1) Immobilization of silane coupling agents reproducible resulted in the formation of initiator thin layers with area densities in the range of 0.446−0.819 group nm^{-2}.

(2) Initiator−grafted silica particles could be successfully utilized to prepare silica-polymer composite materials such as Sil-PSt and Sil-PNVP. The hydrolytic stability of immobilized initiators allowed us to perform polymerization reactions in aqueous medium, as well as to predict that the newly developed systems may be used for the polymerization of numerous (water-soluble) monomers bearing a variety of functional groups.

(3) Present symmetric initiators that enable to attach onto silica surfaces through two anchoring groups have a significant advantage over previously reported AIBN type initiators (Scheme 1); namely, radical fragments do not liberate in the course of polymerization avoiding the formation of large amount of polymers in solution (although a small amount of nonattached polymers were always isolated, most probably derived from different side reactions such as thermal initiation and/or chain transfer to monomer or solvent molecules.)

(4) Solvent free surface-initiated polymerization of *N*-vinyl pyrrolidone resulted in the formation of insoluble polymer domains on the surface that is often considered as the consequence of radical−radical termination in noncontrolled systems.

(5) Our preliminary results aiming at immobilization of **2a**, **2b**, and **2c** onto metal and metal oxide surfaces (e.g., Fe, Fe_2O_3 and Fe_3O_4 nanoparticles) and, furthermore, the noncontrolled feature of the polymerization of different vinylic monomers let us predict the importance of these initiators in the preparation of macroscopic magneto-responsive polymeric gels assisted by intermolecular radical termination.

Acknowledgment. This work was partially supported by Grant-in-Aid for Scientific Research from the Ministry of Education, Culture, Sports, Science and Technology of Japan.

Supporting Information Available: Figures showing ^{1}H NMR spectra of **1** and **2a**−**c**, TGA curve of thermal treated Sil-**2c**, SEM image of Sil-$PNVP_{2c}$ obtained from solvent free polymerization, and ^{1}H NMR spectrum of degrafted PSt. This material is available free of charge via the Internet at http://pubs.acs.org.

References and Notes

(1) Pharm, K. N.; Fullston, D.; Sagoe-Crentsil, K. *J. Colloid Interface Sci.* **2007**, *315*, 123–127.
(2) Glogowski, E.; Tangirala, R.; Russell, T. R.; Emrick, T. *J. Polym. Sci., Part A: Polym. Chem.* **2006**, *44*, 5076–5086.
(3) Li, J.; Wang, J.; Gavalas, V. G.; Atwood, D. A.; Bachas, L. G. *Nano Lett.* **2003**, *3*, 55–58.
(4) Czaun, M.; Rahman, M. M.; Takafuji, M.; Ihara, H. *J. Polym. Sci., Part A: Polym. Chem.* **2008**, *46*, 6664–6671.
(5) Ihara, H.; Okazaki, S.; Ohmori, K.; Uemura, S.; Hirayama, C.; Nagaoka, S. *Anal. Sci.* **1998**, *14*, 349–354.
(6) Czaun, M.; Hevesi, L.; Takafuji, M.; Ihara, H. *Chem. Commun.* **2008**, 2124–2126.

(7) Urman, K.; Otaigbe, J. U. *Prog. Prog. Polym. Sci.* **2007**, *32*, 1462–1498.
(8) Turek, S. L.; Lippincott, J. B. In *Orthopaedics: Principles and Appications*, 2nd ed.; Lippincott Williams & Wilkins: Philadelphia, PA, 1985, pp. 113-136.
(9) Belder, G. F.; ten Brinke, G.; Hadziioannou, G. *Langmuir* **1997**, *13*, 4102–4105.
(10) Szabó, D.; Szeghy, G.; Zrínyi, M. *Macromolecules* **1998**, *31*, 6541–6548.
(11) Szabó, D.; Czakó-Nagy, I.; Zrínyi, M.; Vértes, A. *J. Colloid Interface Sci.* **2000**, *221*, 166–172.
(12) Krenkler, K. P.; Laible, R.; Hamann, K. *Angew. Macromol. Chem.* **1976**, *53*, 101–123.
(13) Ulman, A. *Chem. Rev.* **1996**, *96*, 1533–1554.
(14) Prucker, O.; Rühe, J. *Macromolecules* **1998**, *31*, 592–601.
(15) Cossement, D.; Mekhalif, Z.; Delhalle, J.; Hevesi, L. In *Organosilicon Chemistry VI*,; Auner, N., Weis, J., Eds.; Wiley-VCH: Weinheim, Germany, 2005; Vol. 2, p 999.
(16) Rahman, M. M.; Czaun, M.; Takafuji, M.; Ihara, H. *Chem.—Eur. J.* **2008**, *14*, 1312–1321.
(17) Denes, F. S.; Manolache, S. *Prog. Polym. Sci.* **2004**, *29*, 815–885.
(18) Dekking, H. G. G. *J. Appl. Polym. Sci.* **1965**, *9*, 1641–1651.
(19) Dekking, H. G. G. *J. Appl. Polym. Sci.* **1967**, *11*, 23–36.
(20) Edmondson, S.; Osborne, V. L.; Huck, W. T. S. *Chem. Soc. Rev.* **2004**, *33*, 14–22.
(21) Li, L.; Kang, E.; Neoh, K. *Appl. Surf. Sci.* **2008**, *254*, 2600–2604.
(22) Hansen, N. M. L.; Jankova, K.; Hvilsted, S. *Eur. Polym. J.* **2007**, *43*, 255–293.
(23) Hawker, C. J.; Bosman, A. W.; Harth, E. *Chem. Rev.* **2001**, *101*, 3661–3688.
(24) Weimer, M. W.; Chen, H.; Giannelis, E. P.; Sogah, D. Y. *J. Am. Chem. Soc.* **1999**, *121*, 1615–1616.
(25) Nakatsuka, T. *J. Appl. Polym. Sci.* **1987**, *34*, 2125–2137.
(26) Tsubokawa, N.; Kogure, A.; Maruyama, K.; Sone, Y.; Shimomura, M. *Polym. J.* **1990**, *22*, 827–833.
(27) Zhang, J.; Yang, Y.; Zhao, C.; Zhao, H. *J. Polym. Sci., Part A: Polym. Chem.* **2007**, *45*, 5329–5338.
(28) Prucker, O.; Rühe, J. *Macromolecules* **1998**, *31*, 602–613.
(29) Chuiko, A. A. *Colloids Surf., A* **1993**, *74*, 128.
(30) Meier, L. P.; Shelden, R. A.; Caseri, W. R.; Suter, U. W. *Macromolecules* **1994**, *27*, 1637–1642.
(31) Takei, T.; Kato, K.; Meguro, A.; Chikazawa, M. *Colloids Surf., A* **1999**, *150*, 77–84.
(32) Czaun, M.; Hevesi, L.; Takafuji, M.; Ihara, H. *J. Nanosci. Nanotechn.* **2009**, *9*, 123–131.
(33) von Werne, T.; Patten, T. E. *J. Am. Chem. Soc.* **2001**, *123*, 7497–7505.